ENVIRONMENTAL RESEARCH
COMMUNICATIONS

INCLUSIVE PUBLISHING
TRUSTED SCIENCE

Part of the
ENVIRONMENTAL RESEARCH
SERIES

PURPOSE-LED
PUBLISHING™

First steps towards bridging integrated assessment modeling and high-resolution energy system models: A scenario matrix for a low-emissions sector-coupled European energy system

To cite this article before publication: Ebbe Kyhl Gøtske *et al* 2025 *Environ. Res. Commun.* in press https://doi.org/10.1088/2515-7620/adf60d

First steps towards bridging integrated assessment modeling and high-resolution energy system models: A scenario matrix for a low-emissions sector-coupled European energy system

Ebbe Kyhl Gøtske[1,2,*], Yoga Pratama[3], Gorm Bruun Andresen[1]
Matthew J. Gidden[3,4], Marta Victoria[1,5,6], Behnam Zakeri[3,7]

[1]Department of Mechanical and Production Engineering, Aarhus University, Katrinebjergvej 89F, 8200 Aarhus N, Denmark
[2]Department of Chemical Engineering, Imperial College London, London SW7 2AZ, United Kingdom
[3]International Institute for Applied System Analysis (IIASA), Laxenburg, Vienna, Austria
[4]Center for Global Sustainability, University of Maryland, College Park, MD USA
[5]Novo Nordisk Foundation CO2 Research Center, Aarhus University, Gustav Wieds Vej 10, 8000 Aarhus C, Denmark
[6]Technical University of Denmark (DTU), Kongens Lyngby, Denmark
[7]Institute for Data, Energy, and Sustainability (IDEaS), Vienna University of Economics and Business (WU), Austria
*Corresponding author. E-mail: e.gtske@imperial.ac.uk

Abstract

The rollout of variable renewable energy (VRE) generators, along with the electrification of heating and transport sectors and the production of synthetic fuels for hard-to-abate industries, is a key strategy for mitigating climate change. Energy infrastructure planning models must accurately capture the high spatio-temporal variability of VRE to avoid misestimating their contribution to the power generation. Integrated Assessment Models (IAMs), which operate at a global scale with low spatio-temporal resolution, often rely on simplified VRE representations with predetermined parameters— potentially leading to suboptimal or infeasible scenarios. To address this limitation, we present the first study to impose forced VRE shares in the high-resolution sector-coupled energy system model for Europe, PyPSA-Eur, for the purpose of IAM parameterization. For a nearly net-zero CO_2-emissions system that disregards existing energy infrastructure and builds the optimal capacity mix overnight, we assess the European potential of each technology type across a scenario space with varying forced VRE shares. We derive economic and technical parameters, providing insights applicable to models with lower spatio-temporal resolution.

Introduction

The transition to a sustainable and low-carbon energy future is a paramount global challenge. It necessitates a profound understanding of the interplay between energy

systems and the broader socioeconomic and environmental contexts. Two fundamental tools in this endeavor are Integrated Assessment Models (IAMs) and Energy System Models (ESMs), each possessing unique strengths and limitations. IAMs aim to produce a coherent synthesis of all aspects of climate change, providing a global perspective that encompasses complex global interactions between energy, economy, climate, land use, and more. IAMs are particularly good at capturing the trade-offs between energy scenarios and land-use change and Forestry (LULUCF) at a detaild level to provide feasible estimates of carbon fluxes and other GHG emissions, etc. [1]. Process-based IAMs examine the cost-effectiveness of scenarios, with an explicit representation of the change in the global energy and land-use systems linked with the economy [2]. Following a cost-efficiency approach, which utilizes optimization frameworks to minimize system-wide costs of achieving defined climate targets, they are common tools in assessments of policy decisions. The shortcoming of IAMs is that they typically operate at a high level of spatial and temporal aggregation, which makes them incapable of modeling storage or regional balancing using transmission lines. In addition, they also often lack a proper representation of sector coupling (e.g., direct electrification of heat or EVs and indirect electrification using power-to-X). For this reason, the endogenous computation of optimal capacities and the estimation of integration expenses of variable renewable energy generators is challenged in many IAMs [3, 4, 5]. For instance, some work has shown that IAMs tend to underestimate the supply of variable renewable energy (VRE) sources, comprised of wind energy and solar PV [6].

Contrary to IAMs, ESMs rely on more detailed representations of the energy system at regional and local scale [7, 8, 9, 10]. They incorporate a high level of technical and geographical granularity, enabling more precise assessments of technological and operational aspects. Yet, their limited geographical scope and representation of land use can constrain their ability to capture broader global implications, including bilateral trade of commodities, competition for land and biomass resources, and emissions from LULUCF and agriculture. Given the distinct differences in scope, level of detail, and inclusion of critical system components, integrating the IAM and ESM frameworks offers a promising pathway toward more comprehensive assessments of future energy systems. Linking IAMs with ESMs offers the potential to capitalize on the strengths of both: the global outlook of IAMs and the spatial and technological detail of ESMs. This integration can take multiple forms. For example, prior work has established a backwards (i.e., IAM-to-ESM) uni-directional soft link to test the feasibility of IAM-optimized capacities [5], as well as a bi-directional iterative soft link that maps the Lagrange multipliers between an IAM and ESM until reaching equivalent values [11]. Inspired by the modular integration approach used in the IAM MESSAGEix-GLOBIOM [12], we propose a third methodology. In this study, we implement the first step of a forward uni-directional soft-link, in which parameters are derived from the ESM and later integrated into the IAM. This approach avoids increasing model complexity and reduces the computational burden associated with bi-directional links [11], while also improving feasibility [5]. Using a sector-coupled energy system model, we construct a scenario matrix containing both economic (e.g., market values) and technical (e.g., curtailment) parameters, across a wide range of different wind-solar PV mixes. With this scenario matrix, we intend to capture key features of the energy system that are important to address in a model representation.

In this paper, we explain the outputs for key technologies included in the energy system, while complete data is published for all technologies. Ideally, this dataset

can be used across multiple modeling frameworks as a first step toward improving the representation of renewable energy integration in IAMs. While the main contribution of this paper is the provision of the scenario matrix, we also include an assessment (in Supplementary Note 1) of how variable renewable energy is currently represented in the MESSAGEix-GLOBIOM.

Methods

We use PyPSA-Eur, an open networked model of the European sector-coupled energy system [10, 8], to model an almost fully decarbonized European system (5% net CO_2 emissions relative to 1990 levels), with a 3-hourly resolution and a network of 37 nodes. In PyPSA-Eur, an optimization process involves both capacity expansion and dispatch optimization. The objective is to minimize total system cost while determining optimal energy allocations in time and space, such as the capacity and generation from wind energy and solar PV, in addition to other optimization parameters (see Supplemental Note S2 in [10] for a detailed mathematical description of the model). For this reason, in a default configuration, the proportion of wind and solar PV generation is a result of the optimization. Here, we force the model to deviate from the optimum configuration, in order to trace the impact of integrating renewable energy and collect our findings in a scenario matrix (see Fig. 1). To achieve this, we maintain the 5% CO_2 emissions constraint while forcing wind and solar PV separately into the system (Eq. 1). The European aggregate wind and solar PV capacities are specified exogenously, while the optimization determines the allocation of nodal capacities. The results of PyPSA-Eur are nodal, so that capacity and dispatch are unique in every node. The temporal aggregation from hourly to 3-hourly resolution would tend to overestimate the potential of solar PV due to smoothed feed-in profiles and demand peaks. However, previous work has shown that the error in total system costs with 3-hourly resolution compared to hourly is insubstantial [8]. In this document, we show results which have been aggregated on a European level. For the input time series of available wind energy and solar PV resources, we use weather reanalysis data for 2013, which is considered an average year with regard to its potential yield in solar PV and wind energy [13].

Modeled scenario

Using an overnight greenfield approach, we model a European sector-coupled energy system with a strong policy drive for mitigation strategies (see Table **1** for key assumptions). In this scenario, the system is not allowed to exceed (on an annual balance) 5% of the 1990 historical CO_2 emissions. A direct consequence of this constraint is a strong push for technologies with low CO_2 emissions. In the results section, we provide a sensitivity to the chosen CO_2 emissions constraint. In addition to the power sector, the model also encaptures the decarbonization of the energy consumption in the heating, land transport, shipping, aviation, and industry (including industrial feedstock) sectors with comprehensive carbon management. Sector-coupling brings more flexibility to the system, mainly from energy storage (e.g., pit thermal energy storage in district heating, H_2 storage, and electric vehicle batteries). For electricity storage, we assume Li-ion batteries that can be deployed on utility (high voltage grid) or residential scale (low voltage). On top of this, H_2 produced with electrolyzers can be stored underground (salt caverns) and overground (steel tanks) which, if

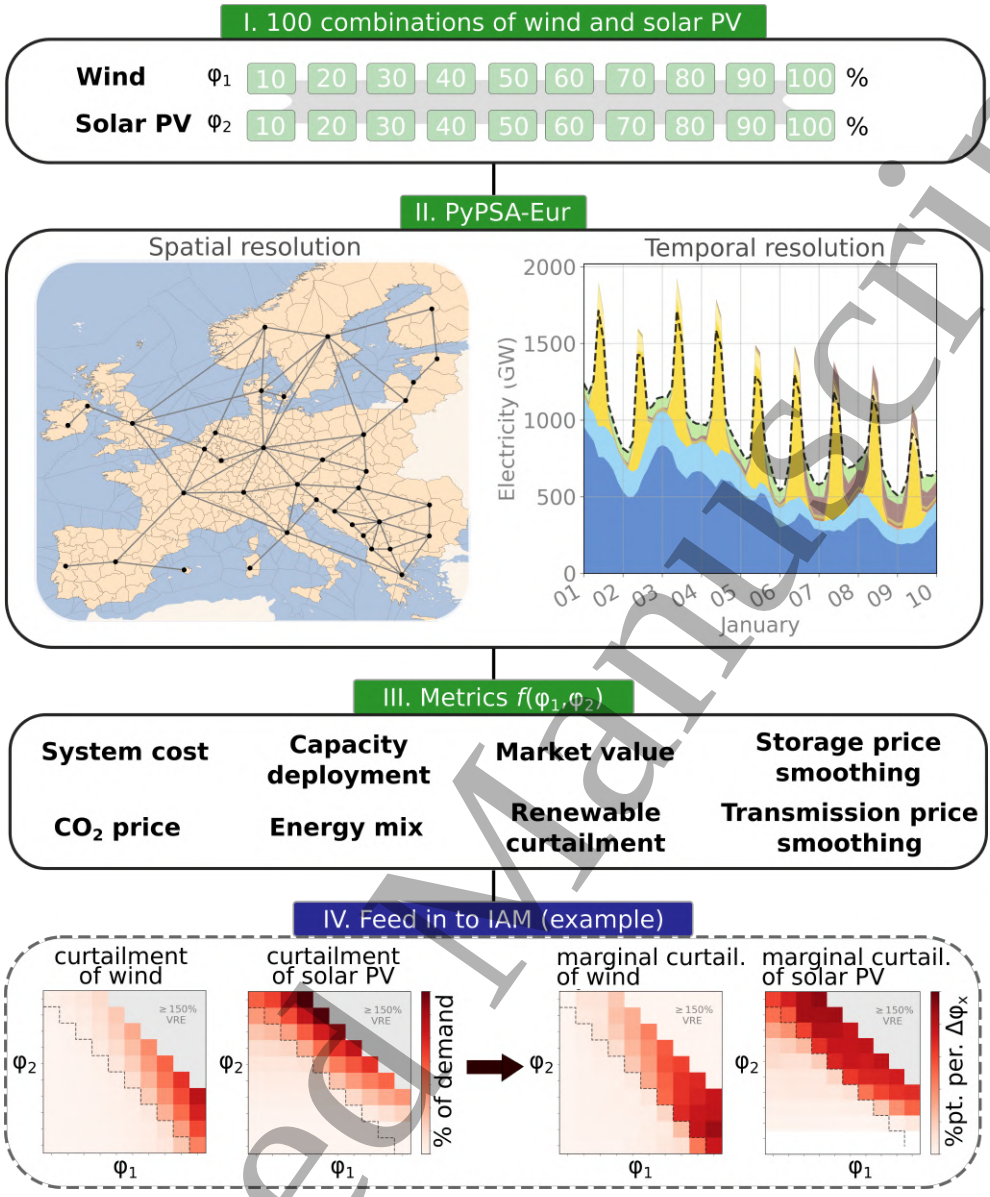

Fig. 1: Workflow. The steps to derive the metrics of interest in this study. The steps include (I) defining the range of wind and solar PV shares of the electricity generation mix, (II) solving the scenarios in the sector-coupled energy system model PyPSA-Eur, and (III) summarizing technical and economic parameters for the defined range. As a potential fourth step (IV), we show the example of deriving one of four renewable integration constraints in the Integrated Assessment Model (IAM) MESSAGEix-GLOBIOM. For a review of the four constraints used in MESSAGEix-GLOBIOM, see Supplementary Note 1.

cost-optimal, can be linked with fuel cells to revert it back to electricity, providing an option for long-duration electricity storage (LDES). For all technologies, we use 2030 cost assumption from the Energy System Technology Data repository v0.5.0 [14] to limit uncertainties related to technology cost evolution.

We include high-voltage transmission lines equivalent to today's capacity and allow the model to expand it further with a maximum of 50% relative to today's volume (sum of the multiplication of capacity and length for all existing transmission lines today). The distribution grid is not modeled, but we assume a distribution grid expansion cost proportional to the deployed low-voltage generation and storage (including EVs). On top of this, the model can also deploy H_2 transmission network. As a final step, we provide a sensitivity assessment of the assumptions of electricity transmission expansion and CO_2 emissions levels.

Table 1: Model settings.

Type	Overnight optimization
Net CO_2 emissions	5% relative to 1990
Capacities	Greenfield (except electricity transmission lines). Existing hydropower capacities are not included.
Time resolution	3-hourly
Network resolution	37 nodes
Renewable energy resolution	370 regions
Weather data	ERA5 reanalysis of 2013 (to model solar PV, we use SARAH-2 irradiance data)
Technology costs	Assumptions according to predictions for 2030
Sectors included	Electricity, heating, industry, land transport, shipping, and aviation
Transmission	Limited to max. 50% volume expansion of today's grid. On top of this, cross-border H_2 pipelines can also be deployed if cost-effective.

Renewable energy share constraint

For a renewable generator R, we define a constraint such that its available annual resources equals a defined share of the electricity demand. Here, the difference between the available resources and the generation from renewable generator R equals curtailed renewable energy. To avoid the artifact of unintended energy losses[1], usually observed as an unintended storage cycling [15, 16], we do not impose a strict binding target on the renewable generation. Instead, we define a target on the available

[1] In hours with renewable generation potential higher than electricity load, the renewable generation constraint forces the renewable generator, instead of curtailing energy, to find alleys of energy losses to fulfill the minimum generation requirement. Here, these alleys can be simultaneous charging and discharging of energy storage which would be a model artifact.

renewable resources, $g_{n,t}^{R,\text{available}}$, which we write as:

$$\sum_{n,t} g_{n,t}^{R,\text{available}} = \sum_{n,t} g_{n,t}^{R} + \sum_{n,t} c_{n,t}^{R} = \varphi^{R} \sum_{n,t} d_{n,t} \tag{1}$$

where $g_{n,t}^{R}$ is the generation of renewable generator R, $c_{n,t}^{R}$ is the renewable curtailment of renewable generator R, φ^{R} is the electricity generation share of renewable generator R, and $d_{n,t}$ is the total electricity demand in node n at time t.

The available renewable resources can be decomposed into a product of the hourly availability factors $\bar{g}_{n,t}^{R,\text{available}}$ and the installed capacity of the renewable generator G_{n}^{R}:

$$\sum_{n,t} \bar{g}_{n,t}^{R,\text{available}} G_{n}^{R} = \varphi^{R} \sum_{n,t} d_{n,t} \tag{2}$$

which reveals that the left-hand side of the equality depends on one decision variable, the nodal capacity G_{n}^{R}. The right-hand side covers the total electricity demand $d_{n,t}$ which includes both exogenous and endogenous sources. The exogenous electricity demand is assumed fixed at historical levels, while an additional electricity demand, i.e., the endogenous demand from direct and indirect electrification, is a variable of the optimization. In our work, the constraint is imposed on wind energy, based on the aggregate of offshore and onshore, and solar PV, based on the aggregate of rooftop and utility scale. The ratio between offshore and onshore wind, as well as the ratio between rooftop and utility-scale solar PV, is determined by the optimization.

Subsequent to the optimization, we calculate the resulting generation share of variable renewable energy (VRE), while accounting for the curtailment in Eq. 1, as:

$$\text{VRE share } \% = \frac{\sum_{n,t} g_{n,t}^{R}}{\sum_{n,s,t} g_{n,s,t}} \tag{3}$$

where $g_{n,s,t}$ is the electricity produced by technology s in node n at time t.

We intend to encapsulate the full range of renewable integration levels, including extreme cases which integrate only wind energy or solar PV, or overbuild renewables such that its potential generation is much higher than the annual electricity demand. Some of them might be unrealistic, practically infeasible, or suboptimal scenarios, but they are useful in this study to indicate the penalty needed on the objective when approaching these extremities.

Renewable energy curtailment

The curtailment of variable renewable energy partially depends on the mismatch between the electricity demand and the renewable generation, the availability of storage (which is limited by the capacity and the filling level) and the available transmission line capacity. With a high spatio-temporal resolution and a model of the high-voltage grid, we can account for these factors. A third aspect that could lead to additional renewable curtailment is the commitments of other generation sources and their ramping constraints. Since our analysis is based on aggregate level and not on plant level, our assessment does not include ramping limit and unit commitment constraints. However, the model assumes long-term market equilibrium (i.e., every asset subject to the optimization needs to operate such that it exactly recovers its costs), which

entails capital intensive power plants to run at a certain capacity factor. This can cause higher levels of unutilized renewable energy at a forced integration level of wind and solar PV.

The order at which curtailment of different technologies occur is determined by the merit order of curtailment. Since the model is built on a cost minimization problem, the model will always choose the generator with the highest marginal costs to be curtailed first. In reality, wind and solar PV have zero marginal costs, but here, we add marginal costs of 0.01 EUR/MWh for wind (both onshore and offshore) and 0.015 EUR/MWh for solar PV (both utility and rooftop) to control the order of curtailment. The marginal costs are small such that they do not affect the objective of the optimization.

We report Europe-aggregated renewable curtailment relative to the electricity demand:

$$\text{curtailed energy } \% = \frac{\sum_{n,t} \left(\bar{g}_{n,t}^{R,\text{available}} G_n^R - g_{n,t}^R \right)}{\sum_{n,t} d_{n,t}} \tag{4}$$

Market values and price smoothing indicators

In this analysis, we develop metrics to describe the economic potential of all types of technologies in the energy system model. For electricity generation technologies, we use the commonly used market value, while for storage and transmission, we describe the potential based on their price smoothing.

1. Market value

The market value indicates the potential revenue of a generation unit per energy produced. Previous work focused on how the market values of renewable power generators decreases while penetrating the energy market, driven by the cannibalization effect (i.e., higher renewable shares decrease the marginal cost of producing electricity, causing revenues of renewable generators to drop [17]). Other studies showed that this effect can be avoided with the adequate policy measure, i.e. setting a CO_2 tax instead of a renewable capacity target [18]. In our analysis, we do not track the change of market values when penetrating today's system. Instead, we consider a scenario in which the system is already close to a full decarbonization, for which we alter the renewable share from very low to very high. In that way, we map the market values in the range of renewable integration levels at a constant CO_2 emissions level, which is different compared to previous work. The market values for generation technologies are calculated as:

$$\text{Market value}_s = \frac{\sum_{n,t} g_{n,s,t} p_{n,t}}{\sum_{n,t} g_{n,s,t}} \tag{5}$$

where $p_{n,t}$ is the locational electricity price, $g_{n,s,t}$ is the generation of every technology s, in every hour t and location n.

2. Price smoothing potential of storage

For each level of renewable integration, our study intends to measure the flexibility required by the model. To its core, flexibility is provided by energy storage. To

measure the required storage, we report the capacity of every technology included in the model. As a supplement to storage capacity, we calculate the potential revenue of each storage type, determined by the price differences between the purchased and the resold power. We refer to this as the storage price smoothing (SPS) indicator. For a storage technology s, this is calculated as:

$$\mathrm{SPS}_s = \frac{\sum_{n,t+} g^{+}_{n,s,t} p^{+}_{n,t} - \sum_{n,t-} g^{-}_{n,s,t} p^{-}_{n,t}}{\sum_n G_{n,s}} \tag{6}$$

where $p^{+}_{n,t}$ is the price of the purchased power $g^{+}_{n,s,t}$, $p^{-}_{n,t}$ is the price of the resold power $g^{-}_{n,s,t}$. Here, we normalize the net revenue by the total deployment $\sum_n G_{n,s}$ of storage technology s.

3. Price smoothing potential of transmission

Similarly, for transmission, we calculate a metric based on the price differences between two nodes, A and B, which we refer to as the transmission price smoothing potential (TPS) for transmission technology s:

$$\mathrm{TPS}_s = \frac{\sum_{l,t} f_{l,t}(p^{\mathrm{A}}_t - p^{\mathrm{B}}_t)}{\sum_l F_l} \tag{7}$$

where $f_{l,t}$ is the power flow of line l at time t. Here, we normalize the net revenue by the total line capacity $\sum_l F_l$.

Results

In our analysis, the system is exposed to both a strong policy push towards decarbonization and a support towards renewable energy technologies proportional to the renewable energy share driven by the constraint in Eq. 2. As this constraint defines the available resources and not the generation, the final renewable fraction of the electricity generation mix depends on the level of curtailment. Fig. 2a indicates a proportionality between the forced integration level and the resulting generation share until the saturation point of 100% is reached. At this point, the marginal contribution of additional generators is low.

The stringent policy on CO_2 emissions pushes out carbon-intensive power generators. Under low VRE integration levels, this leaves room for nuclear power as the primary substitute of wind and solar PV (Fig. 2b). In the nuclear-dominant system, the remaining share is provided mainly by biomass combined heat and power (CHP) plants, supplemented by OCGT and gas CHP. This is, however, a much more expensive solution, which is noticeable from the total system cost (Fig. 2c). Compared to the optimum combination of wind and solar PV, it is 25% more expensive. The figure also shows how, for Europe, wind-dominant systems are less costly than solar PV-dominant systems, in line with many previous papers [19, 20, 21, 8]. The system cost of all combinations of wind and solar PV shows a global minimum at 60% wind and 40% solar PV. An oval shape of near-optimal solutions emerge with similar cost levels but at widely different wind and solar PV combinations, similar to previous research [22]. At a 3% cost increase limit, 15 near-optimal wind-solar combinations emerge, ranging from a 4:1 ratio of wind and solar PV to a 2:3 ratio.

We also show the CO_2 shadow price (Fig. 2d), highlighting combinations that require more policy measures to reach the stringent CO_2 emissions target. The CO_2 shadow price ranges from 350 to 500 EUR/tCO_2. Here, wind-dominant systems and combinations with solar PV require a lower CO_2 tax compared to the remaining scenarios.

Fig. 3a and b show the market values calculated for wind and solar PV. Wind resources generally exhibit higher market values than solar PV. This is primarily attributed to their respective generation profiles: solar PV output is more concentrated and peaks during limited number of hours each day, whereas wind generation tends to be more evenly distributed throughout the day, causing a higher yield per capacity [17]. As previously described, the low VRE share scenarios entail high proportions of nuclear power. As this is a more costly option, the electricity price is higher, which drives up the potential revenue streams for renewable generators. Market values drop proportional to the VRE share due to the cannibalization effect, but does never reach zero, even at very high integration levels (>100%). This is due to the decarbonization policy push, which drives the cross-sectoral electrification, and necessitates more VRE generation capacity in the system, in line with previous studies [18].

When VRE shares are below or equal to 100%, we observe curtailment rates of below 5% and 10% for wind and solar PV (Fig. 3c and d). Over-deployment of VRE (i.e., VRE shares above 100% of the electricity demand) forces renewable generators to have much higher curtailment. In that case, we observe curtailment rates up to 25% and 30%, making the added value of additional renewable generation low when above 100% VRE, and for this reason, the market values of VRE drop dramatically. This explains why these extreme scenarios are not cost-efficient, as shown in Fig. 2c.

In Fig. 4, we first show that the optimal storage capacity is not linear proportional to the share of VRE generation. Instead, it depends largely on the mix of wind and solar PV. Our results reveal the typical pattern of short-duration energy storage and LDES, which is an essential techno-economic aspect of optimal integration of wind and solar PV. Batteries (short-duration storage) complement large penetrations of solar PV, while LDES is only favorable in wind-dominant systems, in line with previous research [24, 25, 26, 27]. Second, we evaluate the economic indicator SPS, for which batteries show lower potential compared to LDES, for the following reason. The bulk energy associated with LDES is much larger due to its lower storage energy capacity cost, making the value per discharge capacity ratio much higher.

In Fig. 5, we evaluate electricity transmission expansion within the range of wind-solar PV combinations. Every scenario utilizes the option of expanding electricity transmission, and it shows some proportionality to the integration of VRE generation. In addition, electricity transmission expansion is noticeably more profitable in wind-dominant systems, based on the transmission price smoothing (TPS) indicator. Such systems have stronger benefit of connecting regions to smoothen spatial imbalances in the renewable energy supply.

For H_2 infrastructure (Fig. 6), we observe distinct behavior between solar- and wind-dominant systems. In solar-dominant systems, the model chooses to ramp up capacity of H_2 electrolyzers and transmission. Conversely, wind-dominant systems have a weakened H_2 grid but a strengthened H_2 storage capacity, compared to solar-dominant cases. This difference is explained by the the seasonal characteristic of wind and solar PV production, where wind is better aligned with the seasonality of

the energy demand. To handle the seasonal mismatch between solar PV production and the energy demand, solar-dominant systems increase the production of H_2 and synthetic oil (Supplementary Fig. 7). Wind-dominant systems show more H_2 storage to balance wind energy droughts, in line with Fig. 4.

When considering the technology mix in the heating supply (Fig. 7), we observe distinct results across the scenario matrix. First, heat pumps (including ground and air source) are the main choice in all combinations, but is highly impacted by the electricity mix as the share of heat pumps varies from 60% to 85%. Generally, an electricity mix with high baseload (which is the case at low VRE scenarios), the system favors a less diverse heating mix. In that case, it is primarily covered with heat pumps (85%) and biomass (10%). Integrating wind and solar PV into the power mix invites different participants into the heating supply. In our model, this includes individual heating units such as resistive heaters and gas boilers (compensated by direct air capture (DAC), see Supplementary Fig. 8), and district heating based on combined heat and power (CHP) units fueled with solid biomass and gas with or without carbon capture (CC). In solar PV-dominant systems, gas boilers have the second highest share (16%) on top of heat pumps (68%) and biomass (10%). For wind-dominant systems, the resistive heaters has the second highest share (14%), on top of heat pumps (63%), biomass (10%), and gas boilers (10%). There are different reasons for why the system tends to deploy more gas boilers or resistive heaters, but the main driver is that it needs low-cost capacity to be activated during cold spells that cause low coefficient of performance of heat pumps. Solid biomass CHP with carbon capture is favored in solar PV-dominant systems. Due to the limited biomass potential, biomass is either used in CHP units or in individual units, depending on the wind-solar PV combination.

In addition to our main results, based on the assumptions listed in Table **1**, we include a second version of the dataset at which we do not allow the expansion of the electricity transmission grid. With this version, it is possible to monitor the system-wide impacts of transmission expansion. Here, we show 4% cost reductions driven by the (maximum 50%) electricity transmission expansion, compared to a case in which we did not allow the expansion of today's grid (Fig. 8, consistent with other research [8]. The cost reductions occur predominantly in wind-dominant systems because the transmission connects better areas with different wind availability. For that reason, transmission expansion pushes the near-optimal space towards higher shares of wind energy. In Supplementary Fig. 9, we show that with transmisison expansion, lower CO_2 taxes are required to facilitate the defined CO_2 emissions limit (5% of 1990 levels) at the given wind and solar PV combination (i.e., the decarbonization needs less policy push because it is more technology-driven). It furthermore eases the curtailment with a few percentage points of both solar PV and wind energy, proving a more efficient utilization of renewable resources. This is partially also helped by a stronger potential of long-duration storage in the wind-dominant systems. As an example, with transmission expansion, the system achieves 95% power generation from wind and solar PV (at the extreme case when forcing 100% wind energy and 10% solar PV into the system), while this is reduced to 91% without it.

While our results are obtained at a specific CO_2 emissions level, it is important to address the sensitivity to this assumption. To do so, we remove the renewable share constraint in Eq. 2 and replace it with a range of CO_2 emissions levels (from 25% to 0% relative to 1990 levels), making the build-out of wind and solar PV a

subject to the optimization. As previously described, using a CO_2 target instead of a renewable share target would lead to more stable market values for renewables, according to literature [18]. In Fig. 9, we show the same. This is consistent with and without transmission expansion, and for a third case in which we include the existing hydropower infrastructure of today. The slight increase in market values of wind energy occur in parallel with a reduced level of wind energy curtailment (see Supplementary Fig. 10-12). To enable the model to reach a full variable renewable power supply, today's capacity of hydropower in Europe was omitted. This choice impacts mostly system costs, since the model finds balancing services elsewhere but with new investments. As shown in Fig. 9, the impact of excluding hydropower on market values of wind and solar PV is insignificant.

Discussion

In this paper, we collect and describe key parameters of a sector-coupled European energy system across a multitude of renewable integration levels. Our study includes an assessment of the required storage and transmission capacities, the market values and revenue indicators of power generators, storage facilities, and transmission lines, as well as the optimal technology mix. Our findings emphasize the importance of accounting for the wind-solar PV mix when considering key integration aspects (including features related sector-coupling, e.g., heating technology mix, H_2 and synthetic gas production, etc.), as they exhibit distinct patterns across the scenario matrix.

Our investigation also serves as a first step in soft-linking ESMs and IAMs. The proceding steps include parameterizing the metrics reported in this study. As we explain in Supplementary Note 1, the parameterization in MESSAGEix-GLOBIOM is based on marginal contributions (e.g., to curtailment) from the increment in the wind or solar PV integration level. For this to work in a linear optimization framework, the metrics considered should be convex across the scenario matrix. This holds for some metrics, while for others, it might not, requiring some convex function approximation. This could induce some error in the parameterization, which should be carefully assessed. Additionally, we observed a diverse system configuration for heating and power-to-X technologies across the wind-solar PV mix. Accounting for this variation in the parameterization, or using it as a bench mark for validation, would enhance the robustness of the soft link. We recommend implementing this framework initially at a European level, to match the geographical domain of this study. For future work, to succeed with a global IAM analysis, our scenario matrices should be adapted to other regions, accounting for differences in VRE potentials and demand profiles.

Here, we mention some limitations of our work. In the heating supply, we assume that generation units can balance each other, similar to electricity generation units. This is a fair assumption for centralized solutions in the urban areas with district heating which usually rely on having a second generation type as a back unit. For individual units, this assumption does often not hold. Moreover, the study was motivated by monitoring the full range of VRE integration. For this reason, we did not account for the existing generation capacity fleet in Europe, e.g., reservoir hydropower, but instead made use of a greenfield approach Integration costs related to the drop in production of existing power plants, as they would need to operate

less, is not accounted for in this data set. Future work should consider how a proper accounting of the starting capacity fleet impacts the results.

Code availability

Our assessment relies on the open energy modeling framework PyPSA and makes use of the model PyPSA-Eur v0.8.0. Costs and technology assumptions are obtained with technology-data v0.4.0. Scripts generated for this project can be accessed from a public repository PyPSA-Eur-Curtailment-Emulator.

Data availability

The data underlying the results presented in this study are openly available from the two repositories ERDA at https://anon.erda.au.dk/cgi-sid/ls.py?share_id=ESLUn4EMQn&current_dir=.&flags=f and Zenodo at 10.5281/zenodo.14831993 [23]. They contain the raw network files, obtained with PyPSA-Eur, and a dataset with the key metrics reported in this study, respectively.

References

[1] R. Jones, R. Leemans, L. Mearns, N. Nakicenovic, A. Pittock, S. Semenov, J. Skea, Ch. 3: Developing and applying scenarios, IPCC Assessment Report 3, WG2 (2001).
URL https://www.ipcc.ch/site/assets/uploads/2018/03/WGII_TAR_full_report-2.pdf

[2] J. Weyant, Some contributions of integrated assessment models of global climate change, Review of Environmental Economics and Policy 11 (1) (2017) 115–137. arXiv:https://doi.org/10.1093/reep/rew018, doi:10.1093/reep/rew018.
URL https://doi.org/10.1093/reep/rew018

[3] P. Sullivan, V. Krey, K. Riahi, Impacts of considering electric sector variability and reliability in the message model, Energy Strategy Reviews 1 (3) (2013) 157–163, future Energy Systems and Market Integration of Wind Power. doi:https://doi.org/10.1016/j.esr.2013.01.001.
URL https://www.sciencedirect.com/science/article/pii/S2211467X13000023

[4] N. Johnson, M. Strubegger, M. McPherson, S. C. Parkinson, V. Krey, P. Sullivan, A reduced-form approach for representing the impacts of wind and solar PV deployment on the structure and operation of the electricity system, Energy Economics 64 (2017) 651–664. doi:https://doi.org/10.1016/j.eneco.2016.07.010.
URL https://www.sciencedirect.com/science/article/pii/S0140988316301827

[5] M. Brinkerink, B. Zakeri, D. Huppmann, J. Glynn, B. Ó Gallachóir, P. Deane, Assessing global climate change mitigation scenarios from

a power system perspective using a novel multi-model framework, Environmental Modelling & Software 150 (2022) 105336. doi:https://doi.org/10.1016/j.envsoft.2022.105336.
URL https://www.sciencedirect.com/science/article/pii/S1364815222000421

[6] M. Victoria, N. Haegel, I. M. Peters, R. Sinton, A. Jäger-Waldau, C. del Cañizo, C. Breyer, M. Stocks, A. Blakers, I. Kaizuka, K. Komoto, A. Smets, Solar photovoltaics is ready to power a sustainable future, Joule 5 (5) (2021) 1041–1056. doi:https://doi.org/10.1016/j.joule.2021.03.005.
URL https://www.sciencedirect.com/science/article/pii/S2542435121001008

[7] C. Breyer, S. Khalili, D. Bogdanov, M. Ram, A. S. Oyewo, A. Aghahosseini, A. Gulagi, A. A. Solomon, D. Keiner, G. Lopez, P. A. Østergaard, H. Lund, B. V. Mathiesen, M. Z. Jacobson, M. Victoria, S. Teske, T. Pregger, V. Fthenakis, M. Raugei, H. Holttinen, U. Bardi, A. Hoekstra, B. K. Sovacool, On the history and future of 100Access 10 (2022) 78176–78218. doi:10.1109/ACCESS.2022.3193402.

[8] F. Neumann, E. Zeyen, M. Victoria, T. Brown, The potential role of a hydrogen network in Europe, Joule 7 (8) (2023) 1793–1817. doi:10.1016/j.joule.2023.06.016.
URL https://www.sciencedirect.com/science/article/pii/S2542435123002660

[9] F. Neumann, J. Hampp, T. Brown, Energy imports and infrastructure in a carbon-neutral european energy system (2024). arXiv:2404.03927.
URL https://arxiv.org/abs/2404.03927

[10] M. Victoria, E. Zeyen, T. Brown, Speed of technological transformations required in Europe to achieve different climate goals, Joule 6 (5) (2022) 1066–1086. doi:https://doi.org/10.1016/j.joule.2022.04.016.
URL https://www.sciencedirect.com/science/article/pii/S2542435122001830

[11] C. C. Gong, F. Ueckerdt, R. Pietzcker, A. Odenweller, W.-P. Schill, M. Kittel, G. Luderer, Bidirectional coupling of the long-term integrated assessment model REgional Model of INvestments and Development (REMIND) v3.0.0 with the hourly power sector model Dispatch and Investment Evaluation Tool with Endogenous Renewables (DIETER) v1.0.2, Geoscientific Model Development 16 (17) (2023) 4977–5033. doi:10.5194/gmd-16-4977-2023.
URL https://gmd.copernicus.org/articles/16/4977/2023/

[12] IIASA, Messageix-globiom documentation (2023).
URL https://docs.messageix.org/projects/global/en/latest/overview/index.html

[13] E. K. Gøtske, G. B. Andresen, F. Neumann, M. Victoria, Designing a sector-coupled european energy system robust to 60 years of historical weather data (2024). arXiv:2404.12178.
URL https://arxiv.org/abs/2404.12178

[14] M. Victoria, K. Zhu, E. Zeyen, T. Brown, Energy system technology data (2020). URL https://github.com/PyPSA/technology-data

[15] M. Kittel, W.-P. Schill, Renewable energy targets and unintended storage cycling: Implications for energy modeling, iScience 25 (4) (2022) 104002. doi:https://doi.org/10.1016/j.isci.2022.104002.
URL https://www.sciencedirect.com/science/article/pii/S2589004222002723

[16] M. Parzen, M. Kittel, D. Friedrich, A. Kiprakis, Reducing energy system model distortions from unintended storage cycling through variable costs, iScience 26 (1) (2023) 105729. doi:https://doi.org/10.1016/j.isci.2022.105729.
URL https://www.sciencedirect.com/science/article/pii/S2589004222020028

[17] L. Hirth, The market value of variable renewables: The effect of solar wind power variability on their relative price, Energy Economics 38 (2013) 218–236. doi:https://doi.org/10.1016/j.eneco.2013.02.004.
URL https://www.sciencedirect.com/science/article/pii/S0140988313000285

[18] T. Brown, L. Reichenberg, Decreasing market value of variable renewables can be avoided by policy action, Energy Economics 100 (2021) 105354. doi:https://doi.org/10.1016/j.eneco.2021.105354.
URL https://www.sciencedirect.com/science/article/pii/S0140988321002607

[19] Optimal future energy mix assessment considering the risk of supply for seven european countries in 2030 and 2050, e-Prime - Advances in Electrical Engineering, Electronics and Energy 5 (2023) 100179. doi:https://doi.org/10.1016/j.prime.2023.100179.
URL https://www.sciencedirect.com/science/article/pii/S2772671123000748

[20] D. Lerede, V. Di Cosmo, L. Savoldi, Temoa-europe: An open-source and open-data energy system optimization model for the analysis of the european energy mix, Energy 308 (2024) 132850. doi:https://doi.org/10.1016/j.energy.2024.132850.
URL https://www.sciencedirect.com/science/article/pii/S0360544224026240

[21] B. Pickering, F. Lombardi, S. Pfenninger, Diversity of options to eliminate fossil fuels and reach carbon neutrality across the entire european energy system, Joule 6 (6) (2022) 1253–1276. doi:https://doi.org/10.1016/j.joule.2022.05.009.
URL https://www.sciencedirect.com/science/article/pii/S2542435122002367

[22] T. T. Pedersen, M. Victoria, M. G. Rasmussen, G. B. Andresen, Modeling all alternative solutions for highly renewable energy systems, Energy 234 (2021) 121294. doi:https://doi.org/10.1016/j.energy.2021.121294.
URL https://www.sciencedirect.com/science/article/pii/S0360544221015425

[23] E. K. Gøtske, Source data (2025). doi:10.5281/zenodo.14831993.

[24] M. Kittel, A. Roth, W.-P. Schill, Coping with the dunkelflaute: Power system implications of variable renewable energy droughts in Europe (2025). arXiv:2411.17683.
URL https://arxiv.org/abs/2411.17683

[25] O. Ruhnau, S. Qvist, Storage requirements in a 100inter-annual variability, Environmental Research Letters 17 (4) (2022) 044018. doi:10.1088/1748-9326/ac4dc8.
URL https://dx.doi.org/10.1088/1748-9326/ac4dc8

[26] M. G. Rasmussen, G. B. Andresen, M. Greiner, Storage and balancing synergies in a fully or highly renewable pan-European power system, Energy Policy 51 (2012) 642–651, renewable Energy in China. doi:https://doi.org/10.1016/j.enpol.2012.09.009.
URL https://www.sciencedirect.com/science/article/pii/S0301421512007677

[27] M. Victoria, K. Zhu, T. Brown, G. B. Andresen, M. Greiner, The role of storage technologies throughout the decarbonisation of the sector-coupled european energy system, Energy Conversion and Management 201 (2019) 111977. doi:https://doi.org/10.1016/j.enconman.2019.111977.
URL https://www.sciencedirect.com/science/article/pii/S0196890419309835

Author contributions

E.K.G. designed the analysis, drafted the manuscript, and contributed to the analysis and interpretation of data. M.J.G., M.V., E.K.G., and B.Z. contributed to the initial idea and conceptualization. B.Z. main-supervised and M.J.G., M.V., Y.P., and G.B.A. co-supervised the project.

Competing interests

The authors declare no competing interests.

Acknowledgements

This work is an outcome of the Young Scientist Summer Program (YSSP), facilitated at the International Institute of Applied System Analysis (IIASA). During this project, E.K.G. was partially funded by the GridScale project supported by the Danish Energy Technology Development and Demonstration Program under Grant No. 64020-2120. The contribution of B.Z. was in part supported by the Austrian Federal Ministry for Innovation, Mobility and Infrastructure (BMIMI) under the endowed professorship for "Data-Driven Knowledge Generation: Climate Action". M.J.G is affiliated with Pacific Northwest National Laboratory, which did not provide specific support for this paper.

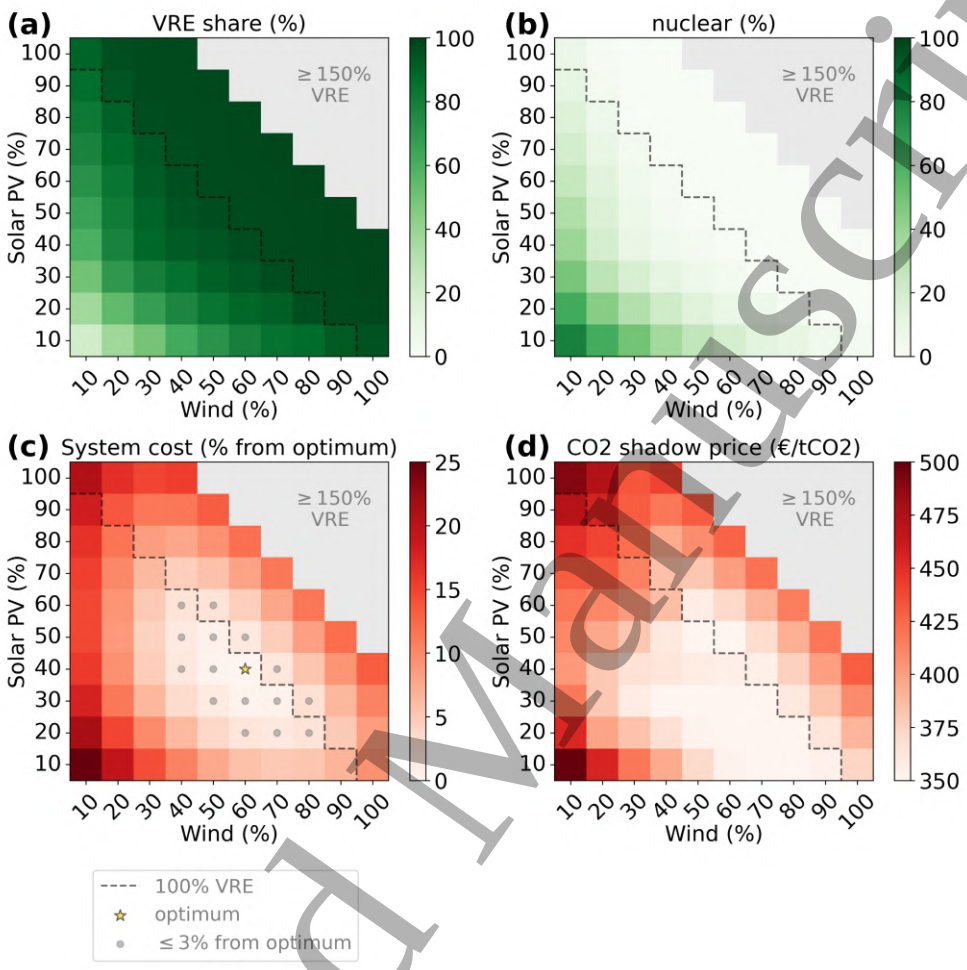

Fig. 2: Renewable electricity share and system cost. (a) Share of electricity generation provided by wind energy and solar PV. (b) Share of electricity generation provided by nuclear power. (c) Total system cost shown as a percentage change from the cost-optimal combination of wind and solar PV. (d) Shadow price of the CO_2 emissions constraint. The dashed line indicates combinations of wind and solar PV in which the generation potential is equal to the annual electricity demand (including electrified demands in heating, industry, and land transport sectors). A cutoff at 150% renewable share is imposed, while data above the cutoff can be found in Source Data file [23].

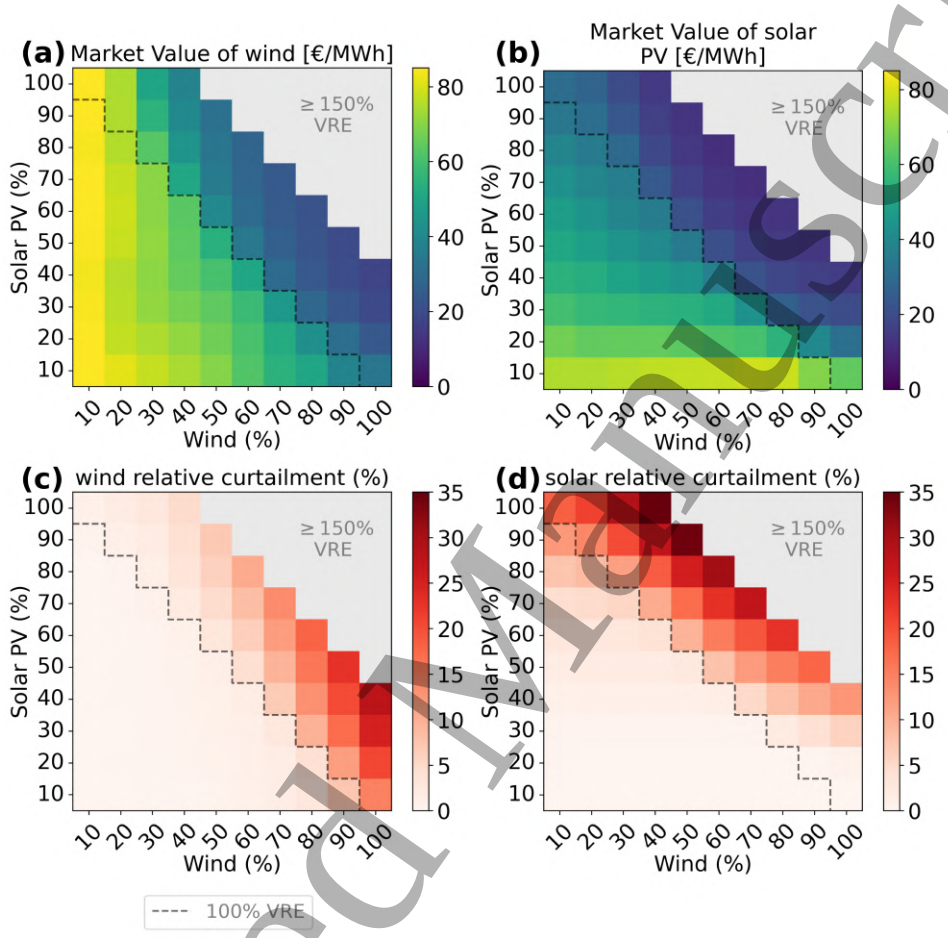

Fig. 3: Market values of variable renewable electricity generators. (a,b) Market values of (a) solar PV and (b) wind energy. (c,d) Curtailment of (c) wind energy and (d) solar PV relative to the annual electricity demand. A cutoff at 150% renewable share is imposed, while data above the cutoff can be found in Source Data file [23].

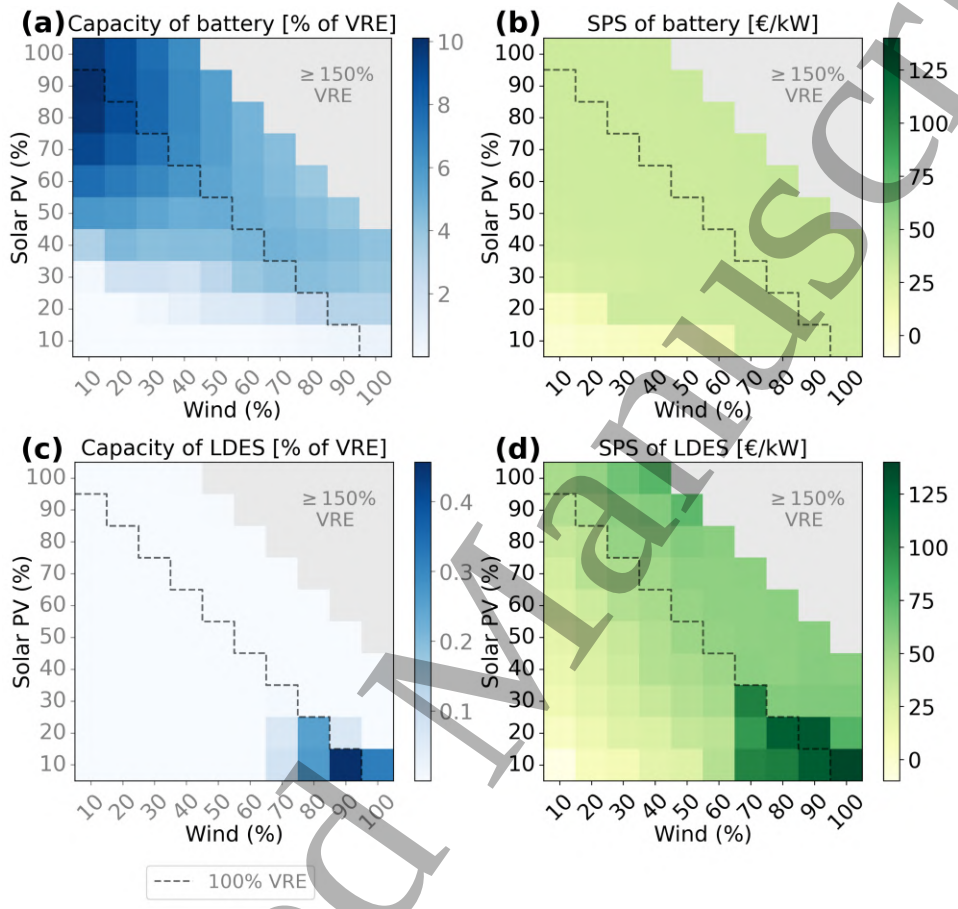

Fig. 4: Storage. (a,c) Discharge power capacity and (b,d) storage price smoothing (SPS) indicator of battery and long-duration electricity storage (LDES). The storage capacities are normalized by the cumulative generation capacity of wind and solar PV to explore the proportionality between the two. Note that we use different scales in each subfigure. A cutoff at 150% renewable share is imposed, while data above the cutoff can be found in Source Data file [23].

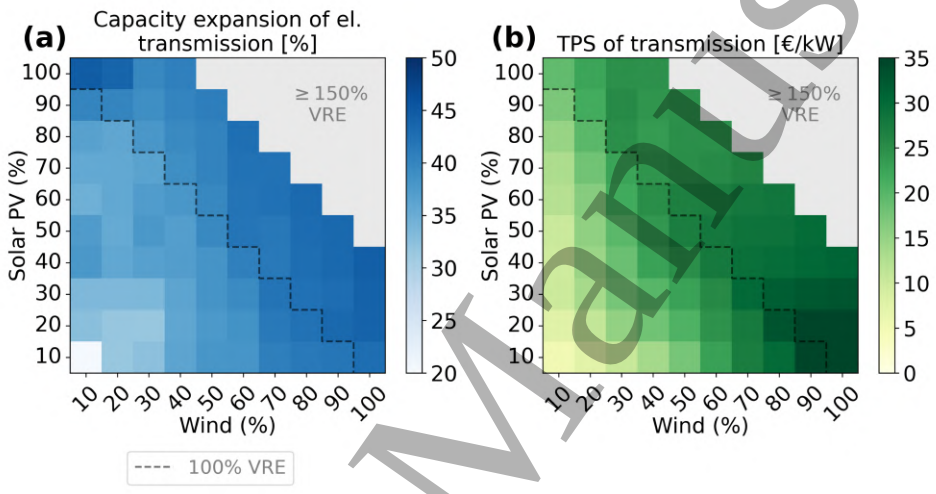

Fig. 5: Transmission. (a) The capacity of electricity transmission relative to today's grid. (b) Transmission price smoothing (TPS) indicator of electricity transmission. Note that we use different scales in each subfigure. A cutoff at 150% renewable share is imposed, while data above the cutoff can be found in Source Data file [23]. See Supplementary Fig. 5 for H_2 transmission.

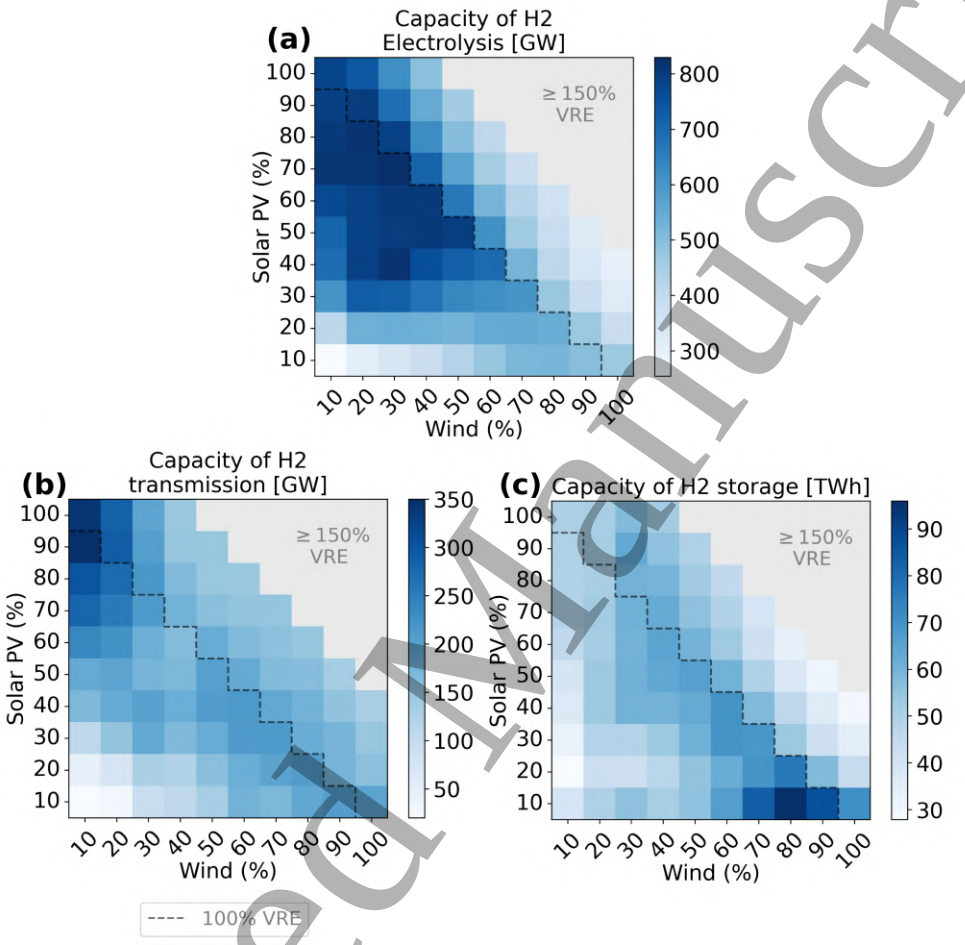

Fig. 6: H_2 infrastructure. Capacity of (a) H_2 electrolyzers, (b) H_2 transmission, and (c) H_2 storage (including both underground and steel tank). Note that we use different scales in each subfigure. A cutoff at 150% renewable share is imposed, while data above the cutoff can be found in Source Data file [23].

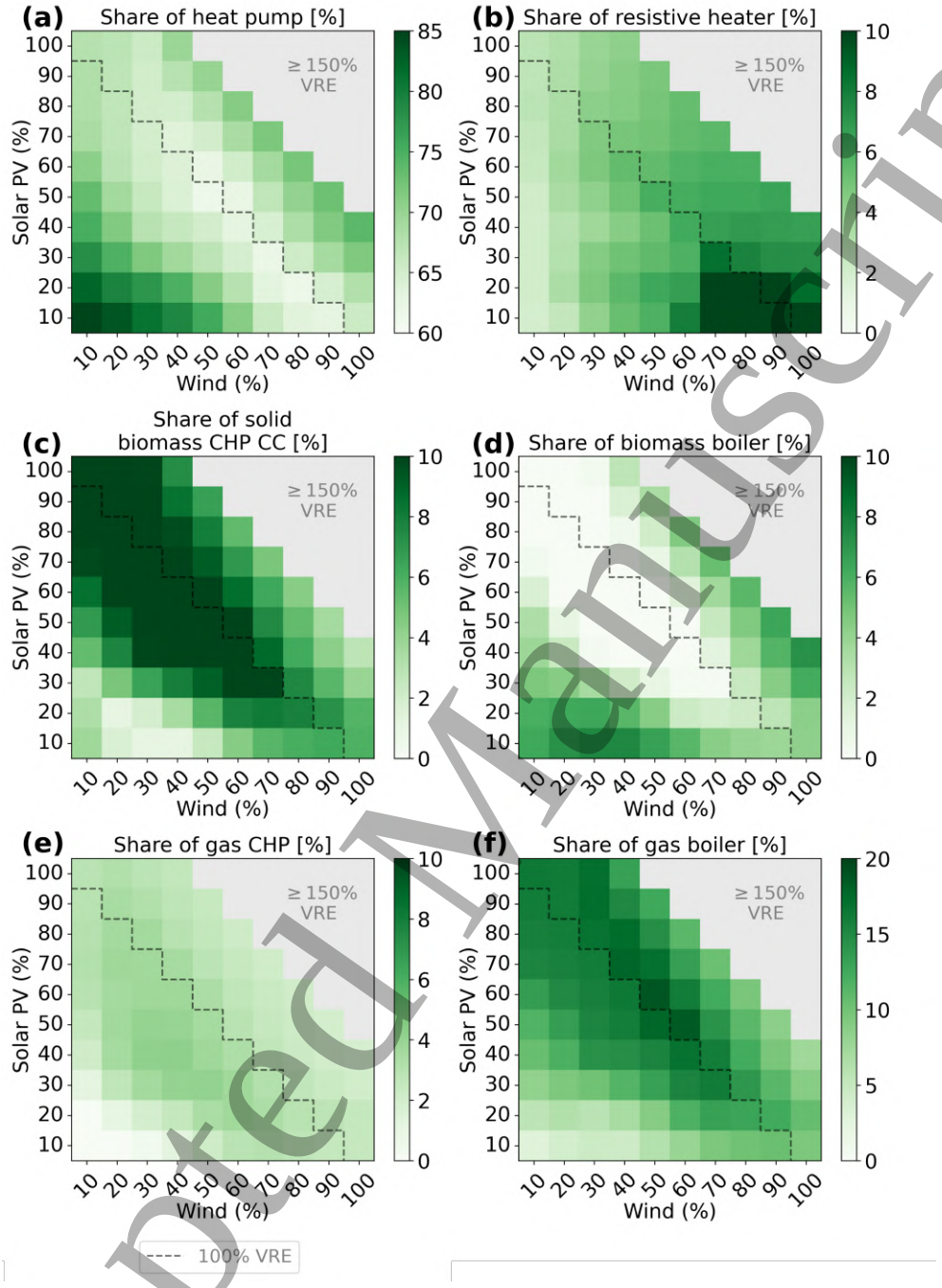

Fig. 7: Heating supply. (a-f) Heating supply mix in percentage for (a) heat pumps, (b) resistive heaters, (c) combined heat and power (CHP) fueled with solid biomass with carbon capture (CC), (d) biomass boiler, (e) CHP fueled with gas, and (f) gas boiler. Note that we use different scales in each subfigure. A cutoff at 150% renewable share is imposed, while data above the cutoff can be found in Source Data file [23].

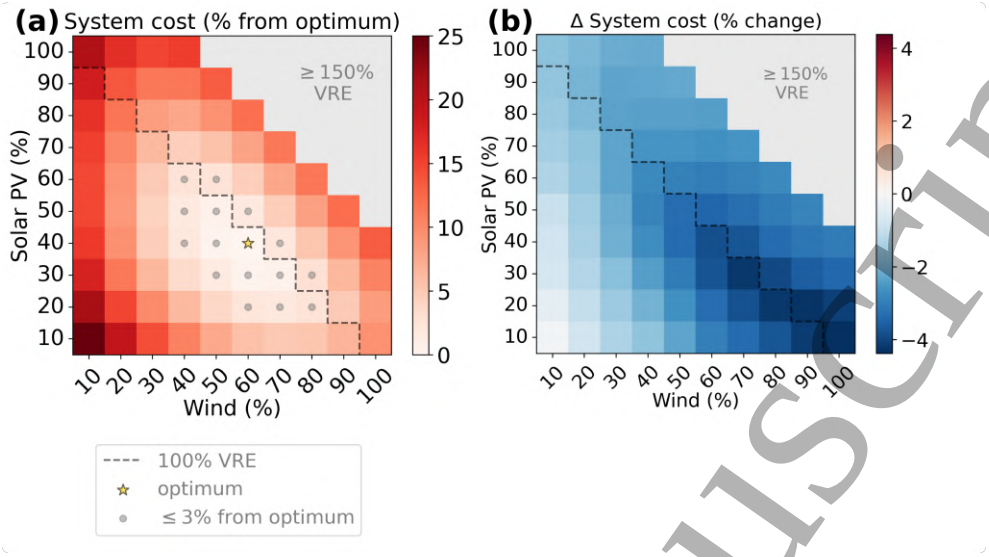

Fig. 8: Impact of transmission expansion. (a) System cost when disallowing an expansion of the electricity transmission grid. (b) Relative change in system cost when allowing an electricity transmission expansion.

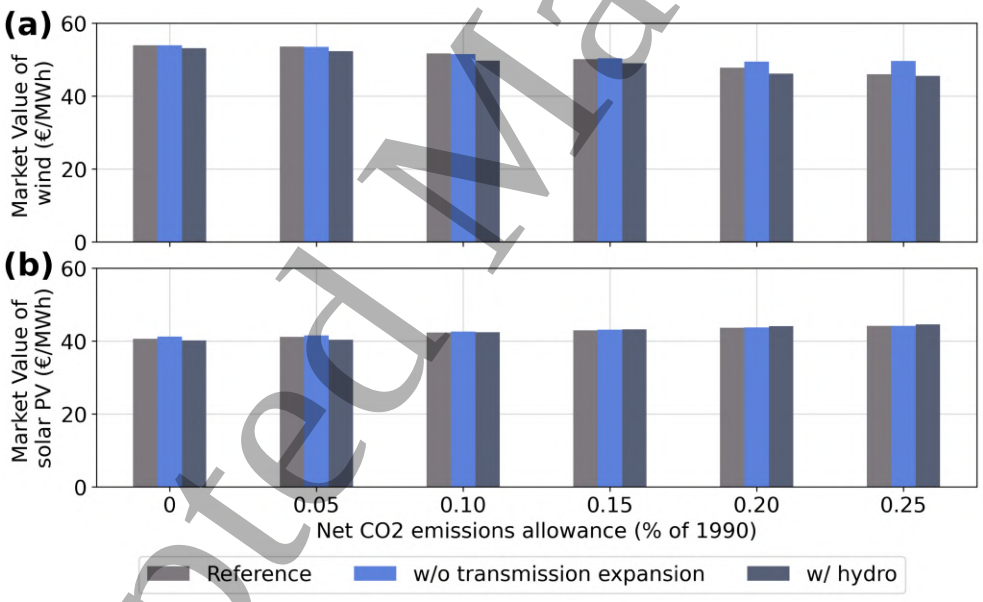

Fig. 9: Market values of wind and solar PV at different CO_2 emissions levels. This is evaluated for three systems, including the one used to generate the primary dataset (reference), one without transmission expansion (w/o transmission exp.), and a third in which we include today's capacity of hydropower (w/ hydro). This part of the analysis disregards the renewable energy share constraint used to generate the primary dataset (Eq. 2).